HYDRO-MAGNETIC FALKNER -SKAN FLUID RHEOLOGY WITH HEAT TRANSFER PROPERTIES

Muhammad AWAIS [1] , Aqsa [2] , Saeed Ehsan AWAN [3,*], Saeed Ur REHMAN [3] , Muhammad Asif Zahoor RAJA [3]

[1]Department of Mathematics, COMSATS University Islamabad, Attock Campus, Attock, Pakistan

[2]Department of Mathematics , Quaid-i-Azam University Islamabad, Pakistan .

[3]Department of Electrical Engineering, COMSATS University Islamabad, Attock Campus, Pakistan
[*] Corresponding author; E-mail: saeed.ehsan@ciit-attock.edu.pk

Abstract: *This article addresses the effects of heat transfer on magnetohydrodynamic (MHD) Falkner-Skan wedge flow of a Jeffery fluid. The continuity, momentum and energy balance equations yield the relevant partial differential equations (PDEs) which are transforms to ordinary differential equations (ODEs) by exploitation of similarity variables. Strength of optimal Homotopy series solutions is practiced to solved analytically the transformed ODEs model of hydro-magnetic Falkner-Skan fluid rheology with heat transfer scenarios. The graphical and numerical illustrations of the result are presented for different interesting flow parameters. Numerical values of Nusselt number are tabulated. It is observed that for the Falkner-Skan rheology, the applied magnetic field acts as a controlling agnet which controls the fluids velocity upto the desired value whereas Debrorah number enhances the fluid velocity.*

Key words*: Falkner-Skan wedge flow, heat transfer, Jeffery fluid, magnetohydrodynamics, OHAM.*

1. Introduction

Prandtl[1] introduced the boundary layer concept for the first time. He described the differences between the viscid and inviscid fluid flow while presented the investigations using boundary layer concept. He concluded that the magnitudes of viscous and inertial forces are same near the solid boundaries. Blasius [2] considered the boundary layer analysis for flow past a flat plate and the results obtained were in an excellent agreement with experimental data. Two-dimensional boundary layer analysis for laminar flow was later discussed by Falkner and Skan [3] and analysis is presented by use of the similarity variables. The solution of the reduced ordinary differential equations (ODEs) was analyzed by Hartree [4]. Thereafter, ample investigations were presented regarding the Falkner-Skan flow under different aspects, few recent studies in this regard are reported in [5-10] and references therein. It is revealed that because of strong nonlinearity, the previous studies were often restricted to viscous fluid and provision of numerical solutions only. The numerical solutions are no doubt lacking to predict the real essence for the analysis of the Falkner-Skan fluid flow problem and hence the struggle to derive analytical results with series solutions is still look promising. It is also recognized now that for different industrial fluids, e.g., artificial fibers, paints, molten plastics, blood at low shear rate, food stuffs, shampoo, polymeric liquids and slurries, exhibit rheological characteristics. The consideration of magnetohydrodynamic (MHD) concepts is significant in metallurgy. An important application of MHD flows lies in the distillation of molten materials from non-metallic inclusion through the applied magnetic flux. Keeping in view all these motivated facts, the present article aims to describe the Falkner-Skan wedge flow of Jeffery fluid for the scenarios MHD and heat transfer. The problem statement and solution is included in the next section. Convergence of the series solution is examined [11-20]. Effects of physical parameters on velocity as well as temperature profiles is described. Comparsion of our achieved results with already published data is also made .Beside these, there are many reported studies in which the dynamics of MHD nanofluidic problems are investigated in diversified fields, see [21-25] and references cited therein.

2. Mathematical Formulation

Let us Consider the two-dimensional Falkner-Skan wedge flow of a Jeffery fluid in the presence of heat transfer. We further taken into account the analysis of a MHD by exerting the magnetic field in a transverse direction of the flow. The surface temperature is denoted by T_w while the ambient value T_∞ is attained when y tends to infinity. The free stream velocity is denoted by $U(x)$. The small magnitude of magnetic Reynolds number is chosen such that we have negligible induced magnetic field as compared to applied magnetic field. In view of the stated assumptions, boundary layer expression that govern the flow and temperature in dimensional form can be mathematical given as [26]:

$$\frac{\partial u}{\partial x}+\frac{\partial v}{\partial y}=0, \tag{1}$$

$$\rho\left(\frac{\partial u}{\partial x}+\frac{\partial v}{\partial x}\right)=-\frac{\partial p}{\partial x}-\sigma B^2(x)u+\left(\frac{\mu}{1+\lambda_1}\right)\frac{\partial^2 u}{\partial y^2}+\left(\frac{\mu\lambda_2}{1+\lambda_1}\right)\left(\frac{\partial u}{\partial x}\frac{\partial^2 u}{\partial y\partial x}+u\frac{\partial^3 u}{\partial y^2\partial x}+\frac{\partial v}{\partial y}\frac{\partial^2 u}{\partial y^2}+v\frac{\partial^3 u}{\partial y^3}\right), \tag{2}$$

$$u\frac{\partial T}{\partial x}+v\frac{\partial T}{\partial y}=\frac{k}{\rho c_p}\frac{\partial^2 T}{\partial y^2}, \tag{3}$$

with horizontal u and vertical v component of the velocities, ρ is the fluid density, ν is the kinematic viscosity, λ_1 is the ratio of relaxation to retardation time, λ_2 is the retardation time, σ denotes the electrical conductivity, B_0 is magnetic field strength, k is the thermal conductivity while c_p is the specific heat .
The relevant boundary conditions can be written as:

$$\begin{aligned} &u=v=0, \quad T=T_w \qquad && y=0,\\ &u\to U(x),\ T\to T_\infty \quad \text{for} && y\to\infty. \end{aligned} \tag{4}$$

Where

$$U(x) = ax^n, \quad B(x) = B_0 x^{(n-1)/2}, \tag{5}$$

If ψ is the stream function then by using the following quantities:

$$\begin{gathered} u = \frac{\partial \psi}{\partial y}, \quad v = -\frac{\partial \psi}{\partial x}, \\ \eta = \sqrt{\frac{n+1}{2}}\sqrt{\frac{U}{\nu x}}y, \; \psi = \sqrt{\frac{n+1}{2}}\sqrt{\nu x U}\, f(\eta), \; u = Uf'(\eta), \quad , \\ v = -\sqrt{\frac{n+1}{2}}\sqrt{\frac{\nu U}{x}}\left[f(\eta) + \frac{n-1}{n+1}\eta f'(\eta) \right], \; \theta(\eta) = \frac{T_w - T}{T_w - T_\infty}, \end{gathered} \tag{6}$$

the equation (1) is satisfied completely while equations (2) to (4) in dimensionless as :

$$\begin{gathered} f''' + (1+\lambda_1)\left(ff'' - M^2(f'-1) + \frac{2n}{n+1}\left(1 - f'^2\right) \right) \\ + \beta\left((n-1) f f''' + \frac{3n-1}{2} f''^2 - \left(\frac{n+1}{2} \right) ff'''' \right) = 0 \end{gathered} \tag{7}$$

$$\theta'' + \Pr f\theta' = 0,, \tag{8}$$

$$\begin{gathered} f(0) = f'(0) = \theta(0) = 0, \\ f'(\infty) = \theta(\infty) = 1, \end{gathered} \tag{9}$$

where primes denotes the differentiation w. r. t η, M is the Hartman number, $\Pr$ is the Prandtl number and β is the Deborah number and are defined as follows:

$$M^2 = \frac{2\sigma B_0^2}{\rho a(1+n)}, \qquad \Pr = \frac{\mu c_p}{\alpha}, \qquad \beta = \lambda_2 \frac{U}{x}.., \tag{10}$$

While another important physical quantity, i.e., skin friction coefficient C_f, is formulated by the following expression :

$$C_f = \frac{1}{\rho (U(x))^2} \tau_{xy}\Big|_{y=0} = \frac{1}{\rho a^2 x^{2n}} \frac{\mu}{1+\lambda_1}\left[\frac{\partial u}{\partial y} + \lambda_2 \left(u \frac{\partial^2 u}{\partial x \partial y} + v \frac{\partial^2 v}{\partial y^2} \right) \right]\Bigg|_{y=0}, \tag{11}$$

The dimensionless form of above expression is

$$C_f = \left(\mathrm{Re}_x\right)^{-1/2}\left[f'' + \beta\left\{ \frac{3n-1}{2} f f'' - \frac{n+1}{2} ff''' \right\} \right]\Bigg|_{\eta=0}, \tag{12}$$

where $R_{e_x} = ax^{n+1}(1+\lambda_1)/\nu$ denotes the local Reynolds number.

For Newtonian fluid, system model equations (7-9) takes the form

$f''' + ff'' + \frac{2n}{n+1}\left(1 - f'^2\right) = 0,$ $\theta'' + \Pr f\theta' = 0,$	(13)
$f(0) = f'(0) = \theta(0) = 0,$ $f'(\infty) = \theta(\infty) = 1,$	(14)

3. Results and Disscussion

The graphical and and numerical illustration of the results are presented here by using the homotopic series results with in convergence region involves the non-zero auxiliary parameters c_0^f and c_0^θ. The optimal values of the parameters c_0^f and c_0^θ can be found by using minimal procedure based on mean value of squared residual errors as :

$E_m^f = \frac{1}{k+1}\sum_{j=0}^{k}\left[N_f\left(\sum_{i=0}^{m} f(\eta)\right)_{\eta = j\delta\eta}\right]^2 d\eta,$	(15)
$E_m^\theta = \frac{1}{k+1}\sum_{j=0}^{k}\left[N_\theta\left(\sum_{i=0}^{m} \theta(\eta)\right)_{\eta = j\delta\eta}\right]^2 d\eta,$	(16)

Where $E_m^t = E_m^f + E_m^\theta$ is the sum of the two residual errors. The minimization of the mean residual errors is carried out through built-in procedure of Mathematica package for solving boundary value problems by taking $d\eta = 0.5$ and k = 20 in equations (15-16). The results of global convergence parameter for different order of the approximation, i.e., m = 2, 4, 6 and 8, are tabulated in Table 1 along with consume time. Accordingly, in Table 2, these results are presented for m = 4, 8 and 12. The decreasing trend is seen in the magnitude of residual errors with increases the parameter m, i.e., the order of approximations but at the cost of significant increase in the computing time. Theh -curves of f and θ are plotted to obtain the reasonable values of h_f and h_θ From Fig. 1 it is found that the range of auxiliary parameters is $-1.7 \le (h_f, h_\theta) \le -0.5$. Fig. 2 is presented just to validate the results. It is found that the residual error in our computation is very small which is nearly equal to zero. In Table 3, numerical results of skin friction coefficient $(\mathrm{Re}_x)^{1/2} c_f$ are presented and these results show that with increase in skin friction coefficient by increasing the parameters η, β and λ_1 whereas the positive magnitudes of M results in decrease of the skin friction coefficient.

The results for variation in η on f' are presented graphically in Fig. 3 which show that by increasing η the values of the velocity profile also increases. The description of streamline illustration for the fluids rheology is presented in Fig. 3. This plots shows the behavior of momentum boundary layer near and far away from the wall. Fig. 4 plots the effect of β on f'. It is found that effects of β and η are quite similar. The effects of M and λ_1 are displayed in the Figs. 5 and 6, respectively. These results show that an increase in the values of M retards the flow whereas λ_1 causes an increase in the velocity profile. Effects of M and Pr on temperature profile θ are shown in the Figs. 7 and 8, respectively. It is noticed that the temperature field increases when M and Pr are increased, while the thickness of thermal boundary layer decreases by increasing M and Pr. Table 5 shows the results of $\theta'(\eta)$ various Prandtl numbers (Pr) and wedge angel parameters, while Table 6 respresnts the results for the laminar boundary layer over a wedge. Tables (5 & 6) Proves the validity of our work, as our results are in good comparsion with already published data,

Table 1*:* Results of optimal convergence on the basis of residual errors

m	c_0^f	c_0^θ	E_m^t	**Time**
2.0	-1.24	-1.07	5.12×10^{-4}	5.73
4.0	-1.16	-0.99	1.58×10^{-5}	66.48
6.0	-1.02	-0.92	2.05×10^{-5}	5170.48
8.0	-0.97	-0.90	5.82×10^{-7}	6281.19

Table 2: Result of individual residual errors for $m=8$ from Table 1

m	E_m^f	E_m^θ	**Time**
4.0	6.14×10^{-5}	4.81×10^{-6}	14.61
8.0	1.95×10^{-7}	8.67×10^{-8}	100.87
12.0	4.30×10^{-9}	2.53×10^{-9}	245.7

Table 3: Result for skin friction coefficients for different phycical parameters

N	β	λ_1	M	$(Re_x)^{1/2} C_f$
0.5	0.2	0.1	0.5	0.85193
1.0	0.2	0.1	0.5	1.14372
1.5	0.2	0.1	0.5	1.32484
0.5	0.0	0.1	0.5	0.84193
0.5	0.2	0.1	0.5	0.89472
0.5	0.4	0.1	0.5	0.92659
0.5	0.2	0.0	0.5	0.17139
0.5	0.2	0.1	0.5	0.25317
0.5	0.2	0.2	0.5	0.31259
0.5	0.2	0.1	0.0	1.16423
0.5	0.2	0.1	0.5	0.91359
0.5	0.2	0.1	1.0	0.31324

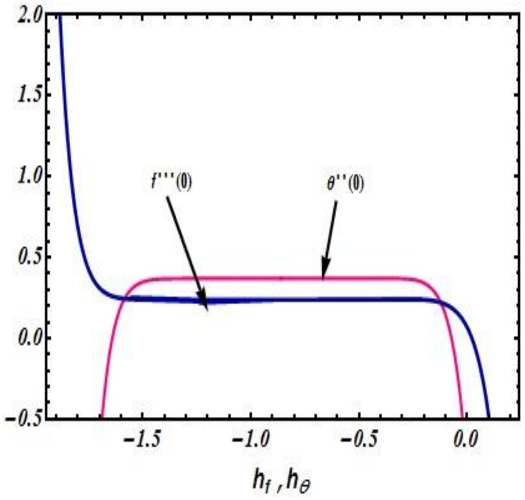

Fig. 1: $h-$**curves for** f **and** θ**.**

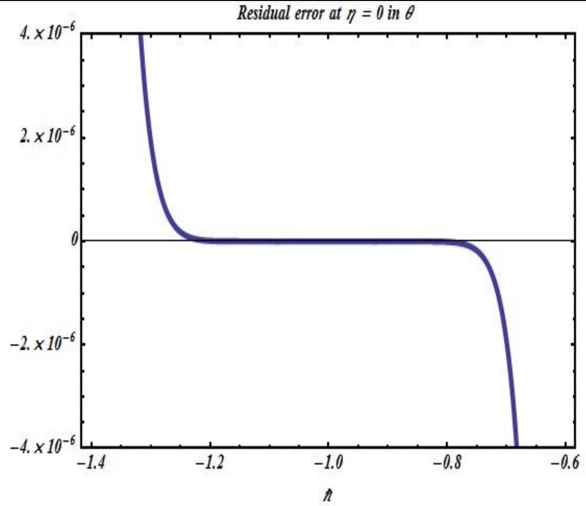

Fig. 2: Residual error in θ**.**

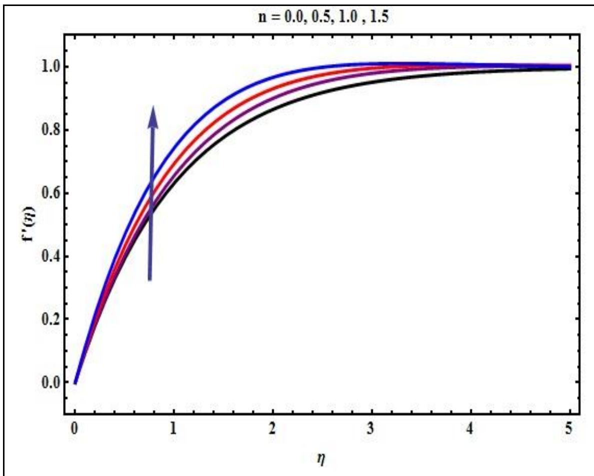

Fig. 3: Result for variation in n **on** f'**..**

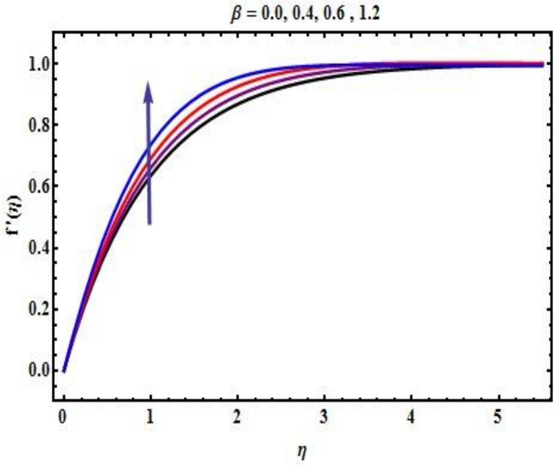

Fig. 4: Result for variation in β **on** f'**..**

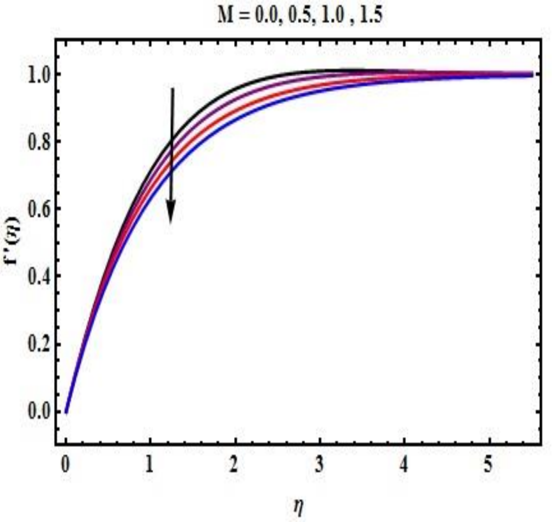

Fig. 5: Result for variation in M **on** f'**.**

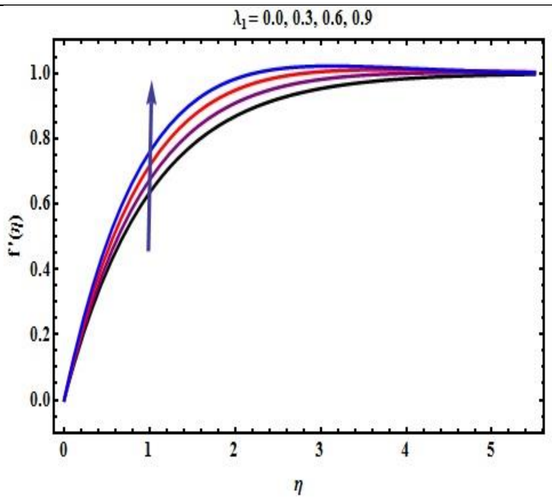

Fig. 6: Result for variation in λ_1 **on** f'**.**

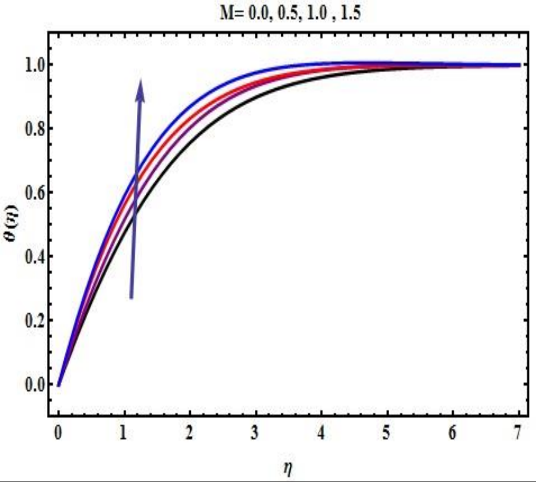

Fig. 7: Result for variation in M on θ.

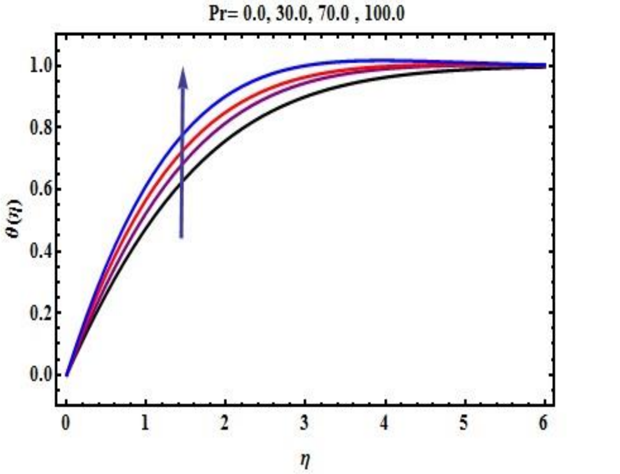

Fig. 8: Result for variation in $\Pr$ on θ.

Table 4: Numerical values of $\theta'(\eta)$ for various Prandtl numbers (Pr) and wedge angel parameters

	$\beta=0$			$\beta=0.3$		
Pr	Present Study	Ref [27]	Ref [28]	Present Study	Ref [27]	Ref [28]
0.1	0.1972	0.1974	0.1980	0.2093	0.2101	0.2090
0.3	0.3047	0.3054	0.3037	0.3285	0.3290	0.3278
0.6	0.3928	0.3923	0.3916	0.4288	0.4290	0.4289
1.0	0.4694	0.4696	0.4696	0.5193	0.5195	0.5195
2.0	0.7976	0.7972	0.5972	0.6688	0.6690	0.6690

Table 5: Comparison of the results for the laminar boundary layer over a wedge

$f''(0)$			
β	Present Study	Ref [27]	Ref [29]
0.0	0.4681	0.4683	0.4696
0.1	0.5877	0.5879	0.5878
0.2	0.6873	0.6873	0.6876
0.4	0.8542	0.8536	0.8549
0.8	1.1189	1.1188	1.1195
1.0	1.2311	1.2313	1.2312

4. **Conclusions**

Following are the concluding remarks for the presented study.

- Nonlinearity parameter "n" enhances the flow. Magnetic field reduces the velocity of fluid.
- By increasing in the intensity of magnetic field "M" decelerates the fluid's velocity and can control the flow field.
- An invrease in the magnetic field increases the momentum boundary layer.
- Retardation time acts as a boosting agent.
- Temperature of the fluid increases with increasing magnetic field.
- The value of the Skin friction coefficient increases by increase in the value of the Deborah number.
- Numerical values of Prandtl number and wedge angel parameter are in close approximation with already published work.
- tNumerical results for the laminar boundary layer over a wedge are are in close approximation with already published work.

In future, one may investigate moderm soft computing based numerical solvers for the solution of hydro-magnetic Falkner-Skan fluidic systems [30-33].

Nomenclature

u,v	Velocity components	MHD	Megnetohydrodynamics
x,y	Axes	ρ	Fluid Density
ψ	Stream Function	β	Deborah Number
c_0^f	Non zero auxiliary parameter	σ	Electrical conductivity
c_0^θ	Non zero auxiliary parameter	C_f	Skin Friction Coffecient
E_m^t	Residual Error Sum	k	Thermal Conductivity
E_m^f	Residual Error	Re_x	Reynolds number
E_m^θ	Residual Error	ν	Kinematic Viscosity
C_p	Specific heat at constant pressure	λ_1	Relaxation Time
M	Hartman Number	λ_2	Retardation time
Pr	Prandtl Number	B_0	Magnetic Field Strength

References:

[1] *Prandtl .L*, "Uber Flussigkeitbewegung bei sehr kleine Reibung", Third International Math. Congress, 1904, pp. 484-491.

[2] *Blasiu. H*, "Grenzschichten in Flussinkeiten mit kleiner Reibung", Z. Angew. Math. Phys., 56 (1908), pp. 1-37.

[3] *Falkneb, V.M. and Skan, S.W.*, Solutions of the boundary-layer equations. The London, Edinburgh, and Dublin. Philosophical Magazine and Journal of Science, 12(1931), pp.865-896.

[4] *Hartee .D.R*, "On an equation occuring in Flakner and Skan's appproximate treatment of the equation of the boundary layer", Proc. Camb. Philos. Soc., 33 (1937), pp. 223-229.

[5] *Zhang, J. and Chen, B.*, 2009. An iterative method for solving the Falkner–Skan equation. Applied Mathematics and Computation, 210(2009), pp.215-222.

[6] *Brynjell, R,. et al.,.* Stability and sensitivity of a cross-flow-dominated Falkner–Skan–Cooke boundary layer with discrete surface roughness. Journal of Fluid Mechanics, 826(2017), pp.830-850.

[7] *Raja, M.A.Z., et al.,* Bio-inspired computational heuristics to study the boundary layer flow of the Falkner-Scan system with mass transfer and wall stretching. Applied Soft Computing, 57(2017), pp.293-314.

[8] *Abbasbandy, S. and Hayat, T*., Solution of the MHD Falkner-Skan flow by homotopy analysis method. Communications in Nonlinear Science and Numerical Simulation, 14(2009), pp.3591-3598.

[9] *Khan, M., et al*.,. Effects of melting and heat generation/absorption on unsteady Falkner-Skan flow of Carreau nanofluid over a wedge. International Journal of Heat and Mass Transfer, 110(2017), pp.437-446.

[10] *Alizadeh, E., et al.,* Solution of the Falkner-Skan equation for wedge by Adomian decomposition method", Comm. Nonlinear Sci. Numer. simulat., **14** (2009) 724-734.

[11] *Liao .S.J*, "Beyond perturbation: introduction to the homotopy analysis method" London/Boca Raton (FL): Chapman & Hall/CRC Press; (2003).

[12] *Pfeffer, T. and Pollet, L.,* A stochastic root finding approach: the homotopy analysis method applied to Dyson–Schwinger equations. New Journal of Physics, 19(2017), p.043005.

[13] *Elsaid, A., et.al*., Analytical Approximate Solution of Fractional Wave Equation by the Optimal Homotopy Analysis Method. European Journal of Pure and Applied Mathematics, 10(2017), pp.586-601.

[14] *Noroozi, M.J., et al*., A new approximate-analytical method to solve non-Fourier heat conduction problems. Kuwait Journal of Science, 44(2017).

[15] *Sabir, M.M*., 2018. Electrohydrodynamic flow solution in ion drag in a circular cylindrical conduit using hybrid neural network and genetic algorithm. Kuwait Journal of Science, 45(2018).

[16] Dirican, S. and Musul, H.. Comparison of effects of two different feeding rations (high feed rates and limited) on growth of rainbow trout in rectangular concrete pools culture conditions of Susehri in Turkey. Kuwait Journal of Science, 44(2017).

[17] *Khan, J.A., et al*., Design and application of nature inspired computing approach for nonlinear stiff oscillatory problems. Neural Computing and Applications, 26(2015), pp.1763-1780.

[18] *Awais, M., et al.,* Generalized magnetic effects in a Sakiadis flow of polymeric nano-liquids: Analytic and numerical solutions. Journal of Molecular Liquids, 24(2017), pp.570-576.

[19] *Awais, M., et al.,* Hydromagnetic mixed convective flow over a wall with variable thickness and Cattaneo-Christov heat flux model: OHAM analysis. Results in physics, 8(2018), pp.621-627.

[20] *Awais, M., et al*. Nanoparticles and nonlinear thermal radiation properties in the rheology of polymeric material. Results in Physics, 8(2018), pp.1038-1045.

[21] Awan, S.E., *et al*., Numerical Treatment for Hydro-magnetic Unsteady Channel Flow of Nanofluid with Heat Transfer. Results in Physics. 9(2018) ,pp. 1543-1554.

[22] Siddiqa, S., et al., Thermal radiation therapy of biomagnetic fluid flow in the presence of localized magnetic field. International Journal of Thermal Sciences, 132(2018), pp.457-465.

[23] Awan, S.E., et al., Dynamical analysis for nanofluid slip rheology with thermal radiation, heat generation/absorption and convective wall properties. AIP Advances, 8(2018),7, p.075122.

[24] Awais, M., ., *et al., 2018*. Numerical and analytical approach for Sakiadis rheology of generalized polymeric material with magnetic field and heat source/sink. Thermal Science, https://doi.org/10.2298/TSCI180426284A.

[25] T. Hayat, *et al*.,, Similar solution for three-dimensional flow in an Oldroyd-B fluid over a stretching Surface, International Journal for Numerical Methods in Fluids, 70 (2012) 851-859.

[26] *Awais, M., et al*, Newtonian heating, thermal-diffusion and diffusion-thermo effects in an axisymmetric flow of a Jeffery fluid over a stretching surface. Brazilian Journal of Chemical Engineering, 32(2015), pp.555-561.

[27] *Barania, H., et al.,* Flow analysis for the Falkner–Sken wedge flow. Current Science, (2012) pp.169-177.

[28] *White, F. M.,* Viscous Fluid Flow, McGraw-Hill, New York, 1991, 2nd edn, pp. 242–249

[29] *Kuo, B.L.,* Heat transfer analysis for the Falkner–Skan wedge flow by the differential transformation method. International Journal of Heat and Mass Transfer, 48(2005), pp.5036-5046.

[30] Raja, M.A.Z., Mehmood, A., ur Rehman, A., Khan, A. and Zameer, A., Bio-inspired computational heuristics for Sisko fluid flow and heat transfer models. Applied Soft Computing, 71(2018), pp.622-648.

[31] Ahmad, I., et al., Neuro-evolutionary computing paradigm for Painlevé equation-II in nonlinear optics. The European Physical Journal Plus, 133(2018), p.184.

[32] Sabir, Z., et al., Neuro-heuristics for nonlinear singular Thomas-Fermi systems. Applied Soft Computing, 65(2018), pp.152-169.

[33] Ahmad, I., et al., Intelligent computing to solve fifth-order boundary value problem arising in induction motor models. Neural Computing and Applications, 29(2018), pp.449-466.